A rapid computational approach identifies SPICE1 as an Aurora kinase substrate

Jovana Deretic, Alastair Kerr, and Julie P. I. Welburn*
Wellcome Trust Centre for Cell Biology, School of Biological Sciences, University of Edinburgh, Edinburgh EH9 3JR, Scotland, UK

ABSTRACT **Aurora kinases play a major role in mitosis by regulating diverse substrates. Defining their critical downstream targets is important in understanding Aurora kinase function. Here we have developed an unbiased computational approach to identify new Aurora kinase substrates based on phosphorylation site clustering, protein localization, protein structure, and species conservation. We validate the microtubule-associated proteins Clasp2, Elys, tubulin tyrosine ligase-like polyglutamylase residues 330–624 and spindle and centriole associated protein 1, residues 549–855 (SPICE1), as Aurora A and B kinases substrates in vitro. We also demonstrate that SPICE1 localization is regulated by Aurora kinases during mitosis. In the absence of Aurora kinase activity, SPICE1 remains at centrioles but does not target to the spindle. Similarly, a nonphosphorylatable SPICE1 mutant no longer localizes to the spindle. Finally, we show that misregulating SPICE1 phosphorylation results in abnormal centriole number, spindle multipolarity, and chromosome alignment defects. Overall, our work indicates that temporal and spatial Aurora kinase–mediated regulation of SPICE1 is important for correct chromosome segregation. In addition, our work provides a database-search tool that enables rapid identification of Aurora kinase substrates.**

Monitoring Editor
Laurent Blanchoin
CEA Grenoble

Received: Aug 30, 2018
Revised: Nov 8, 2018
Accepted: Nov 20, 2018

INTRODUCTION

Phosphorylation of hundreds of proteins by a small number of mitotic kinases drives correct chromosome segregation (Dephoure *et al.*, 2008; Olsen *et al.*, 2010). The Aurora kinase family plays an important role in cell division and the maintenance of genomic integrity. In particular, Aurora A and B kinases control mitotic events to ensure genomic stability (reviewed in Welburn and Jeyaprakash, 2018). Aurora kinases are serine/threonine kinases that share a common substrate preference. Consequently, the substrate specificity and the function of Aurora kinases A and B are largely governed by their subcellular localization (Fu *et al.*, 2009; Hans *et al.*, 2009). During mitosis, Aurora A is tethered at centrosomes, where it controls bipolar spindle assembly and maintenance. In contrast, Aurora B is bound to chromosomes and then restricted to centromeres during metaphase before relocating to the spindle midzone during anaphase and midbody and the cell cortex during cytokinesis. Aurora B promotes chromosome condensation and biorientation, controls the attachment of kinetochores to microtubules, and regulates abscission during cytokinesis (reviewed in Welburn and Jeyaprakash, 2018).

Proteomic studies indicate that Aurora kinases phosphorylate a large number of substrates during mitosis (Kettenbach *et al.*, 2011; Santamaria *et al.*, 2011). Yet the direct identification of Aurora kinase substrates and their subsequent functional analysis remains difficult. Typically Aurora kinases phosphorylate serines and threonines that fit the consensus site [KR]-[KR]-[S/Tp]-[Φ], although the substrate selectivity at P+1 is weaker (Cheeseman *et al.*, 2002; Kettenbach *et al.*, 2011) (Figure 1A). Phosphorylation often occurs in unstructured regions of a protein, disrupting the region electrostatically and creating or abolishing binding sites. Some of the known substrates are Kif2c/MCAK (mitotic centromere-associated kinesin), components of the KMN network (Knl1, Mis12 complex, Ndc80 complex) (Ndc80, Dsn1, and Knl1), other kinetochore components (CENP-C, CENP-E, INCENP), and centrosomal proteins such as Tpx2 (Andrews *et al.*, 2004; DeLuca *et al.*, 2006; Okada *et al.*, 2006; Kim *et al.*, 2010; Welburn *et al.*, 2010).

To predict novel physiological substrates of Aurora kinases, we generated a computational tool to identify Aurora kinase substrates based on the consensus sequence for the Aurora kinase (further described under *Materials and Methods*). This search tool allows

This article was published online ahead of print in MBoC in Press (http://www.molbiolcell.org/cgi/doi/10.1091/mbc.E18-08-0495) on November 28, 2018.

*Address correspondence to: Julie P. I. Welburn (Julie.Welburn@ed.ac.uk).

Abbreviations used: MCAK, mitotic centromere-associated kinesin; SPICE1, spindle and centriole associated protein 1.

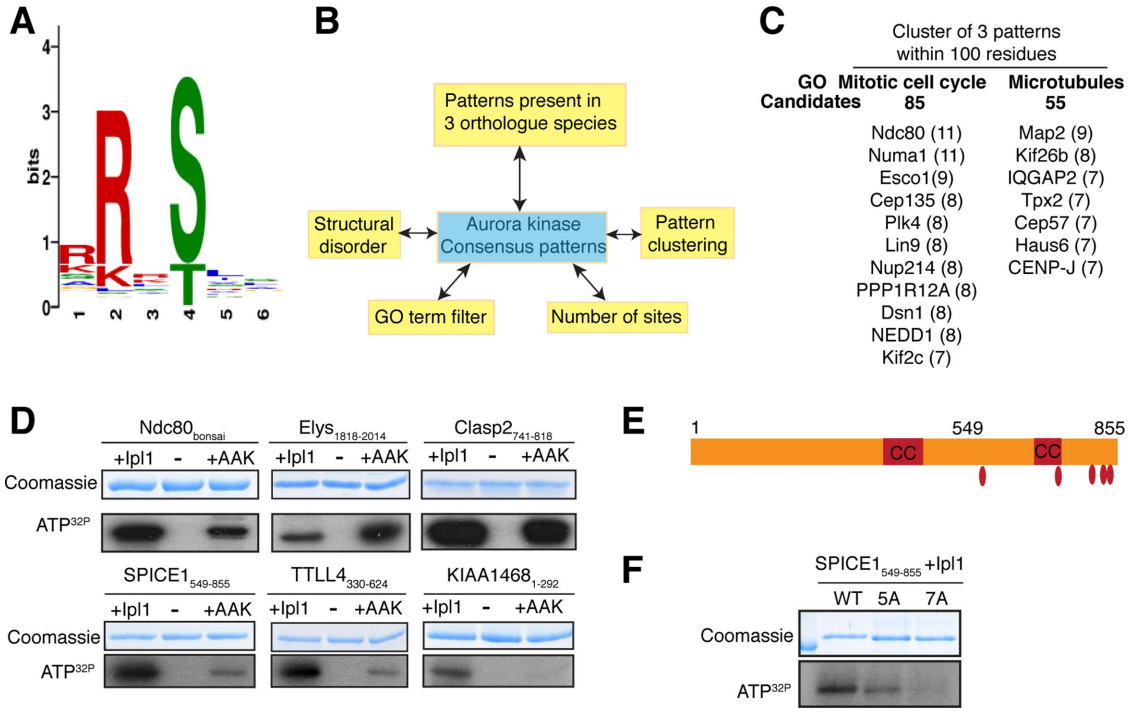

FIGURE 1: Bionformatics and validation of candidate substrates by in vitro phosphorylation assays. (A) Consensus phosphorylation motif and sequence bias in validating putative phosphorylation sites of Aurora kinases. Motif logo was generated using http://meme-suite.org (Bailey *et al.*, 2009) by submitting 13-amino-acid-long sequences of known Aurora kinase phosphorylation sites. (B) Schematic diagram of bioinformatic design with nonlinear flow of available filters. (C) Example of list of candidates derived from bioinformatics based on the presence of at least three consensus patterns within a 100-amino-acid region of a protein and based on biological process or localization (GO term). Numbers in brackets show predicted phosphorylation sites. (D) Coomassie-stained gels and corresponding autoradiogram showing the protein levels and levels of phosphorylation for the Ndc80 bonsai complex, $ELYS_{1858-2014}$ (UniProt ID Q8WYP5), $CLASP2_{741-818}$ isoform X15 (NCBI XP_006713112.1), $SPICE1_{549-855}$ (Q8N0Z3), $TTLL4_{330-624}$ (Q14679), and $KIAA1468_{1-292}$ Cra_a isoform (Q96ES0), respectively. Short constructs of candidate substrates containing predicted phosphorylation were mixed with Ipl1 (yeast Aurora B kinase), buffer only, or Aurora A kinase in the presence of ^{32}P-ATP. (E) Schematic diagram of SPICE1 showing the position of the coiled-coil domains (cc, red) and the predicted phosphorylation sites (red disks). (F) Coomassie-stained gel and corresponding autoradiogram showing SPICE1 (fragment 549–855), $SPICE1_{5A}$, and $SPICE1_{7A}$ in the presence of Ipl1 and ^{32}P-ATP.

filtering of potential substrates using various parameters such as the number of these consensus sites clustered within a region, presence and category in the Gene Ontology database, level of conservation across species, and level of disorder in the region containing the patterns. These parameters are controlled by the user interface and offers great search flexibility. We validated a number of predicted substrates in vitro using kinase phosphorylation assays. We also confirmed the spindle and centriole associated protein 1, residues 549–855 (SPICE1), as a novel substrate of Aurora kinases in cells. Overall, this computational tool enables a rapid search of the proteome to identify novel Aurora substrates and will be an excellent resource for the research community.

RESULTS AND DISCUSSION

To search for novel Aurora kinase substrates, we established a species filter so that a potential substrate can be selected depending on Aurora kinase sites present in only up to three metazoan species (humans, zebrafish, and chickens) (Figure 1, A and B). We also enabled our bioinformatics tool to select data on the basis of predicted structural disorder, number of Aurora consensus sites clustered with a small region, tissue specificity, and gene ontology (GO) terms. We designed an interface that allows the search and classification of potential substrates across species based on any combination of these parameters (Figure 1, B and C).

We tested our approach by identifying known substrates in our search. We applied a species filter so that a potential substrate was only selected if at least three Aurora kinase sites were present in three metazoan species (humans, zebrafish, and chickens). Ndc80 and Kif2c (also known as MCAK) are known to be phosphorylated by Aurora A and B on multiple sites (Andrews *et al.*, 2004; Cheeseman *et al.*, 2006; DeLuca *et al.*, 2006). Searching for substrates that contained at least three consensus sites clustered within a 100-amino-acid stretch, we found Ndc80 contains 11 Aurora consensus sites, including multiple sites in its N terminus previously identified (Cheeseman *et al.*, 2006; DeLuca *et al.*, 2006). Human Kif2c/MCAK is predicted to have seven Aurora consensus sites, four of which have been previously identified as Aurora B kinase sites and two as Aurora A kinase sites (Andrews *et al.*, 2004; Zhang *et al.*, 2008). Searching for substrates that contained at least three Aurora consensus sites clustered within a 100-amino-acid stretch, we found 85 and 55 candidates with GO terms mitotic cell cycle and microtubules, respectively. The top candidates are listed in Figure 1C. A number of these proteins have been previously identified as Aurora substrates, validating our approach. We then focused on candidates that were known to localize close to

Aurora A and Aurora B kinases in mitosis but had not so far been identified as Aurora substrates.

To test whether our bioinformatics tool enabled reliable identification of novel Aurora substrates, we selected five mitotic candidates that were predicted as Aurora substrates containing clusters of phosphorylation sites (at least three phosphorylation sites within 100 amino acids) but not previously reported as Aurora kinase substrates. We purified these recombinantly expressed proteins and used in vitro kinase assays to test whether they were phosphorylated by Aurora A and the yeast Aurora B kinase Ipl1. As a positive control, we used the Ndc80 bonsai complex, which is phosphorylated in the N terminus by Aurora kinases (Cheeseman *et al.*, 2006; DeLuca *et al.*, 2006; Ciferri *et al.*, 2008; Ye *et al.*, 2015). Ndc80 was phosphorylated by both Aurora A and Ipl1 (Figure 1D). Then we tested the nucleoporin Elys and microtubule binding protein Clasp2, which both localize to kinetochores in mitosis. Elys and Clasp2 were predicted to have 26 and 19 phosphorylation sites in total. We recombinantly expressed and purified domains of Elys (residues 1818–2014) and Clasp2 (residues 741–818), containing multiple predicted phosphorylation sites (4 and 5, respectively). Both appeared strongly phosphorylated by Aurora kinases (Figure 1D). Interestingly, the Clasp2 domain is in the microtubule-binding glutamate-arginine–rich region, containing two EB-binding SXIP motifs and heavily regulated by glycogen synthase kinase 3 (GSK3) phosphorylation (Kumar and Wittmann, 2012). Aurora kinases A and B also phosphorylate tubulin tyrosine ligaselike polyglutamylase residues 330–624 (TTLL4), which regulates microtubule posttranslational modifications (Figure 1D). We found that Aurora kinases A and B also phosphorylate the C terminus of SPICE1 (Figure 1, D and E). Finally, the role of KIAA1468 is not known; however, we found this protein had sequence similarities to the microtubule-binding protein tumor overexpressed gene (TOG), comprising a number of TOG-like domains. We found that the N terminus of KIAA1468 (residues 1–292) was phosphorylated by both Ipl1 and Aurora A kinase.

We focused further on SPICE1 as an Aurora substrate and generated a nonphosphorylatable $SPICE1_{5A}$, with the predicted phosphorylated residues mutated to alanines (residues T557, S738, T780, S797, and S810; Figure 1E). T557 has also previously been found phosphorylated in vivo (Moritz *et al.*, 2010; Hornbeck *et al.*, 2015). Additionally, two sites neighboring the predicted phosphorylation sites: T798 and S811 also match the Aurora consensus closely and have been reported to be phosphorylated in mass spectrometry studies (Dephoure *et al.*, 2008; Moritz *et al.*, 2010; Hornbeck *et al.*, 2015). Aurora kinases are capable of phosphorylating consecutive target residues such as the TSS motif in INCENP (Bishop and Schumacher, 2002; Honda *et al.*, 2003). Thus these sites were included to make a $SPICE1_{7A}$ construct (Figure 1E). Phosphorylation of $SPICE1_{5A}$ by the yeast Aurora B kinase Ipl1 was strongly reduced, while phosphorylation of $SPICE1_{7A}$ was almost abolished, indicating that the seven sites were Aurora kinase phosphorylation sites in vitro (Figure 1F). In total, our bioinformatics approach predicts Aurora kinase substrates in vitro accurately and enables the discovery of new mitotic substrates of Aurora kinases.

We then investigated whether these substrates were regulated by Aurora kinases in vivo and focused on SPICE1. Since the C terminus of SPICE1 is phosphorylated in vitro by Aurora kinases (Figure 1F), we examined the role of the C terminus of SPICE1 on its cellular localization in mitosis. Full-length SPICE1 targets to the spindle and centrioles, in agreement with previous work, while $SPICE1_{444\text{-}855}$ failed to localize (Figure 2A) (Archinti *et al.*, 2010). $SPICE1_{1\text{-}550}$ localized to the spindle and centrioles (Figure 2A) (Archinti *et al.*, 2010), however its spindle localization was weakened when compared with full-length SPICE1 (Figure 2, B and C). This indicates that the C terminus of SPICE1 enhances its targeting to the spindle, despite not targeting to microtubules directly (Figure 2). $SPICE1_{1\text{-}550}$ failed to cause centriole amplification whilst the overexpression of full-length SPICE1 caused supernumerary centrioles (Figure 2, C and D), indicating that the C terminus of SPICE1 contributes positively to control of centriole number.

We established functional assays to test how Aurora kinases may regulate SPICE1 function through C-terminal phosphorylation. We first generated an inducible SPICE1 knockout cell line using CRISPR/Cas9-mediated gene targeting (McKinley and Cheeseman, 2014). After 96 h of Cas9 induction, we examined the levels of SPICE1 depletion (Supplemental Figure S1, A and B). SPICE1 depletion was largely successful (Supplemental Figure S1B). In control cells, 82% of untreated cells had a total of four centrioles, as marked by centrin foci staining (Supplemental Figure S1C). The number of centrioles was increasingly abnormal in doxycycline-treated SPICE1-knockout cells with 48% cells having more or less than four centrin foci (Supplemental Figure S1C). Chromosomes showed increased misalignment, 51% misaligned in SPICE1-knockout cells, while only 25% of untreated cells displayed misaligned chromosomes (Supplemental Figure S1D). There were also spindle organization defects and multipolarity in 31% of SPICE1-knockout cells, while only 7% of untreated cells displayed multipolar spindles (Supplemental Figure S1E).

We then used silencing RNA (siRNA) to deplete SPICE1 and confirm the knockout phenotype observed for SPICE1 (Supplemental Figure S1, F and G). While 90% of control cells displayed four centrioles, only 65% of SPICE1 RNA interference (RNAi)-depleted cells had four centrioles (Supplemental Figure S1H) and 27% of cells had fewer than four centrioles. Respectively, 8 and 48% of control and SPICE1-RNAi-depleted cells displayed misaligned chromosomes (Supplemental Figure S1I). We found that on successful depletion of SPICE1, there was an increase in frequency of multipolar spindles, with 21% of cells displaying a multipolar spindle phenotype (Supplemental Figure S1J). Overall, the phenotype of SPICE1 knockout was similar to the published RNAi-based SPICE1 knockdown and our SPICE1 siRNA depletion (Archinti *et al.*, 2010).

Since SPICE1 is phosphorylated in vitro by Aurora kinases, we wanted to test whether SPICE1 localization is regulated by Aurora kinases in cells. Thus we examined the localization of SPICE1 on Aurora kinase inhibition using small molecule Aurora B- and Aurora A-specific inhibitors ZM447439 and MLN8237, respectively (de Groot *et al.*, 2015). Histone H3 is an established Aurora B kinase substrate. First, we confirmed that ZM447439 treatment was successful in inhibiting Aurora kinase B at a concentration where it has minimal activity on Aurora A, as Histone H3 was no longer phosphorylated after ZM447439 treatment (de Groot *et al.*, 2015; DeLuca *et al.*, 2018). Histone H3 phosphorylation persisted after MLN8237 treatment (Supplemental Figure S2A), indicating that MLN8237 inhibited specifically Aurora A kinase as previously showed (Ye *et al.*, 2015). In the absence of Aurora kinase inhibition, green fluorescent protein (GFP)-SPICE1 localizes to the centrioles and the spindle. After a 1.5 h treatment with ZM447439 and MLN8237, GFP-SPICE1 targeting to the spindle was strongly reduced (Figure 3, A and B). However, SPICE1 could still localize to centrioles. Similarly, the spindle localization of endogenous SPICE1 was also strongly reduced in the absence of Aurora kinase activity but not its centriole localization (Figure 3, C and D). Next we wanted to test whether the nonphosphorylatable $SPICE1_{SA}$ and phosphomimetic $SPICE_{SE}$ mutants displayed any changes in localization with respect to SPICE1. GFP-$SPICE1_{5A}$ and GFP-$SPICE1_{7A}$ were strongly

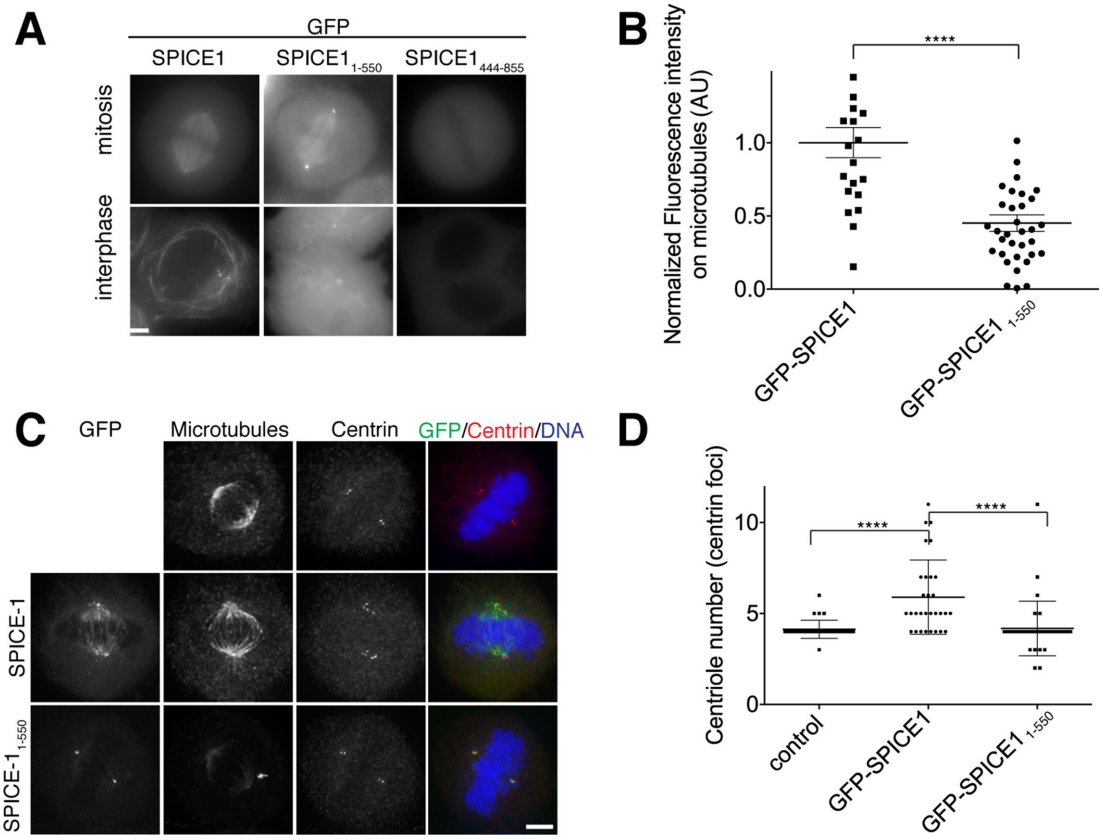

FIGURE 2: The C terminus of SPICE1 regulates SPICE1 targeting to microtubules and centriole number in cells. (A) Representative live-cell images of HeLa cells transfected with GFP-SPICE1, GFP-SPICE1$_{1\text{-}550}$, and GFP-SPICE1$_{444\text{-}855}$ in mitosis and interphase. (B) Quantification of GFP signal intensity on microtubules. Each data point represents one cell for which a background-corrected mean integrated intensity of the GFP signal on MTs was normalized to GFP-SPICE1 fluorescence intensity (GFP-SPICE1 $n = 21$; GFP-SPICE1$_{1\text{-}550}$, $n = 34$). The error bars represent the SEM. The p value for Student's t test is ****<0.0001. (C) Representative deconvolved maximum z-projections of the HeLa cells transiently expressing GFP-SPICE1 or GFP-SPICE1$_{1\text{-}550}$, immunostained with anti–β-tubulin and anti-centrin antibodies, and stained with Hoechst for DNA. (D) Quantification of centriole number based on centrin staining in HeLa cells transiently expressing GFP-SPICE1 or GFP-SPICE1$_{1\text{-}550}$ (control $n = 31$; GFP-SPICE1 $n = 30$; GFP-SPICE1$_{1\text{-}550}$ $n = 34$). The error bars represent the SD. The p values for Kolmogorov–Smirnov test are ****<0.0001. Scale bars, 5 μm.

reduced on the spindle as expected, whereas GFP-SPICE1$_{5E}$ and GFP-SPICE1$_{7E}$ remained present on the spindle with levels similar to GFP-SPICE1 (Figure 4, A and B). In total, these results indicate that Aurora kinase phosphorylation contributes to regulating the targeting of SPICE1 to the spindle.

SPICE1 is a centriole- and spindle-associated protein implicated in regulating centriole number and length, as well as a role in spindle organization (Archinti *et al.*, 2010; Comartin *et al.*, 2013). However, the molecular mechanism underpinning its function is not known. To test whether constitutive phosphorylation could affect SPICE1 function, we examined the spindle morphology, centriole number, and chromosome alignment in the presence of the SPICE1 mutants and in the absence of endogenous SPICE1. First, we established that siRNA-resistant GFP-SPICE1 could rescue chromosome misalignment defects, multipolar spindles, and centriole number defects (Figure 4 and Supplemental Figure S1F). Of control cells, 96% had bipolar spindles. Similarly, 94, 97, and 100% of cells expressing GFP-SPICE1, GFP-SPICE1$_{5A}$, and GFP-SPICE1$_{7A}$ displayed bipolar mitotic spindles (Figure 4C). In the absence of endogenous SPICE1, rates of chromosome alignment in GFP-SPICE1$_{5A}$ and GFP-SPICE1$_{7A}$ transfected cells were similar to control cells and siRNA-resistant GFP-SPICE1–rescued cells (Figure 4, A and D). The number of centrin foci observed for control cells was also similar to that of GFP-SPICE1, GFP-SPICE1$_{5A}$, and GFP-SPICE1$_{7A}$, with 90% control cells having four centrioles and 86, 83, and 88% for GFP-SPICE1, GFP-SPICE1$_{5A}$, and GFP-SPICE1$_{7A}$, respectively (Figure 4, A and E). In contrast, GFP-SPICE1$_{5E}$ and GFP-SPICE1$_{7E}$ transfected cells displayed an increase in chromosome alignment defects and in multipolar spindles, similarly to SPICE1-depleted cells. GFP-SPICE1$_{5E}$ and GFP-SPICE1$_{7E}$ transfected cells displayed more multipolar spindles, 15 and 17% of cells, respectively, while 21% of SPICE1-depleted cells had multipolar spindles (Figure 4, A and C). There was an accumulation of mitotic cells, and less than 50% of the cells displayed aligned chromosomes in both GFP-SPICE1$_{5E}$– and GFP-SPICE1$_{7E}$–transfected cells, reminiscent of SPICE1-depleted cells (Figure 4, A and D). GFP-SPICE1$_{5E}$– and GFP-SPICE1$_{7E}$–expressing cells also displayed an increase in the abnormal centriole number similarly to SPICE1-depleted cells, as marked by the number of centrin foci (Figure 4E). Only 70 and 52% of GFP-SPICE1$_{5E}$– and GFP-SPICE1$_{7E}$–expressing cells had four centrioles, respectively (Figure 4, A and E). Overall, the phenotypes observed in GFP-SPICE1$_{5E}$– and GFP-SPICE1$_{7E}$–expressing cells were very similar to that of SPICE1-depleted cells. Aurora phosphorylation of SPICE1 plays a role in down-regulating the activity of SPICE1. In total, our results

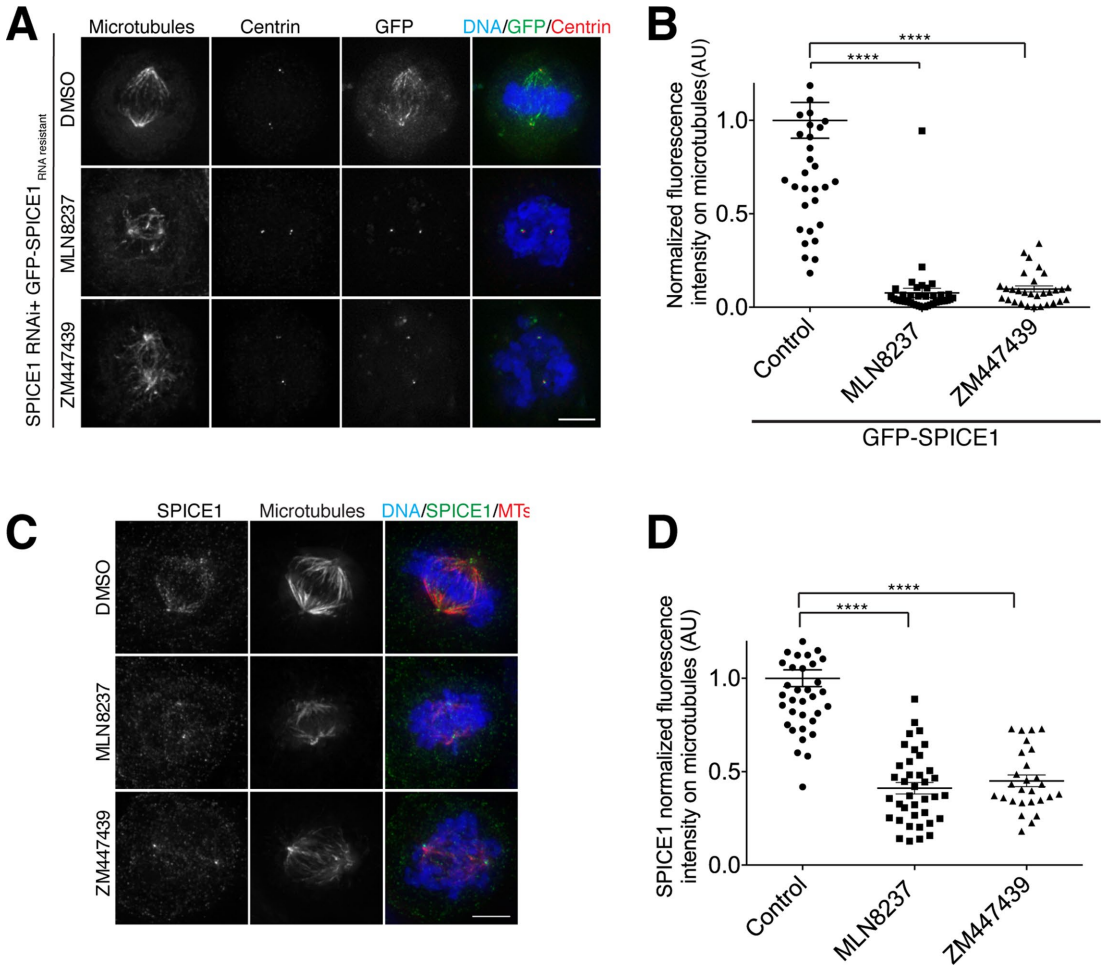

FIGURE 3: Aurora kinases regulate the cellular localization of SPICE1 to microtubules. (A) Representative deconvolved maximum z-projections of SPICE1-depleted HeLa cells and transiently transfected with GFP-SPICE1 after treatment with dimethyl sulfoxide (DMSO) (control), Aurora A inhibitor MLN8237, or Aurora B inhibitor ZM447439. Cells were immunostained with anti–β-tubulin and anti-centrin antibodies and stained with Hoechst for DNA. (B) Scatter plot showing the average normalized GFP fluorescence intensity on microtubules relative to the GFP fluorescence on microtubules in DMSO-treated metaphase cells. Each data point represents background-corrected integrated intensity of the GFP signal on microtubules (DMSO $n = 40$; MLN8237 $n = 38$; ZM447439 $n = 30$). (C) Representative deconvolved maximum z-projections of HeLa cells treated with DMSO, MLN8237, or ZM447439 and immunostained with anti-SPICE1 and anti–β-tubulin antibodies. (D) Scatter plot showing normalized SPICE1 fluorescence intensity on microtubules relative to the fluorescence intensity of SPICE1 on microtubules in DMSO-treated metaphase cells. Experiment repeated twice (DMSO $n = 42$; MLN8237 $n = 38$; ZM447439 $n = 27$). The error bars represent the SEM. The p values for one-way ANOVA tests are reported: ****$p < 0.0001$. Scale bars, 5 μm.

indicate that the dynamic phosphorylation of SPICE1 is essential for correct centriole number, spindle architecture, and chromosome segregation.

Large proteomic approaches and peptides array studies have identified many mitotic substrates (Dephoure *et al.*, 2008; Dulla *et al.*, 2010; Mok *et al.*, 2010). However, the kinase responsible for the phosphorylation is not necessarily associated with these sites. Additionally, phosphopeptides are often missed, as they are less easily ionized than other peptides. To identify new Aurora kinase substrates, we have used a computational approach and developed a searchable database for Aurora kinase phosphorylation consensus sites, with criteria that the user can select (Figure 1B). Selection factors include both the number of sites and phosphorylation site clustering: many Aurora kinase phosphorylation sites are found in close proximity to each other as demonstrated for Kif2c/MCAK and the KMN network (Andrews *et al.*, 2004; Welburn *et al.*, 2010; Zaytsev *et al.*, 2015). Many functionally important phosphorylation sites are conserved across species and are located in disordered regions, and both features can be used here as search parameters. Finally, Gene Ontology is also used to classify the candidate proteins based on their function and localization, focusing on cell division and the cell cycle due to the mitotic role of Aurora kinases. Applying these criteria to mitotic and spindle associated proteins, we could correctly predict a number of known Aurora kinase substrates such as Ndc80, Numa1, Tpx2, Dsn1, and Kif2c/MCAK (Figure 1C) (Andrews *et al.*, 2004; Cheeseman *et al.*, 2006; DeLuca *et al.*, 2006; Fu *et al.*, 2015; Gallini *et al.*, 2016). From the other candidates identified in our study, we tested whether the nucleopore- and kinetochore-localized Elys, plus-end associated Clasp2, spindle- and centriole-associated SPICE1, tubulin polyglutamylase TTLL4, and an unknown protein KIAA1468 were Aurora kinase substrates. All were successfully phosphorylated by

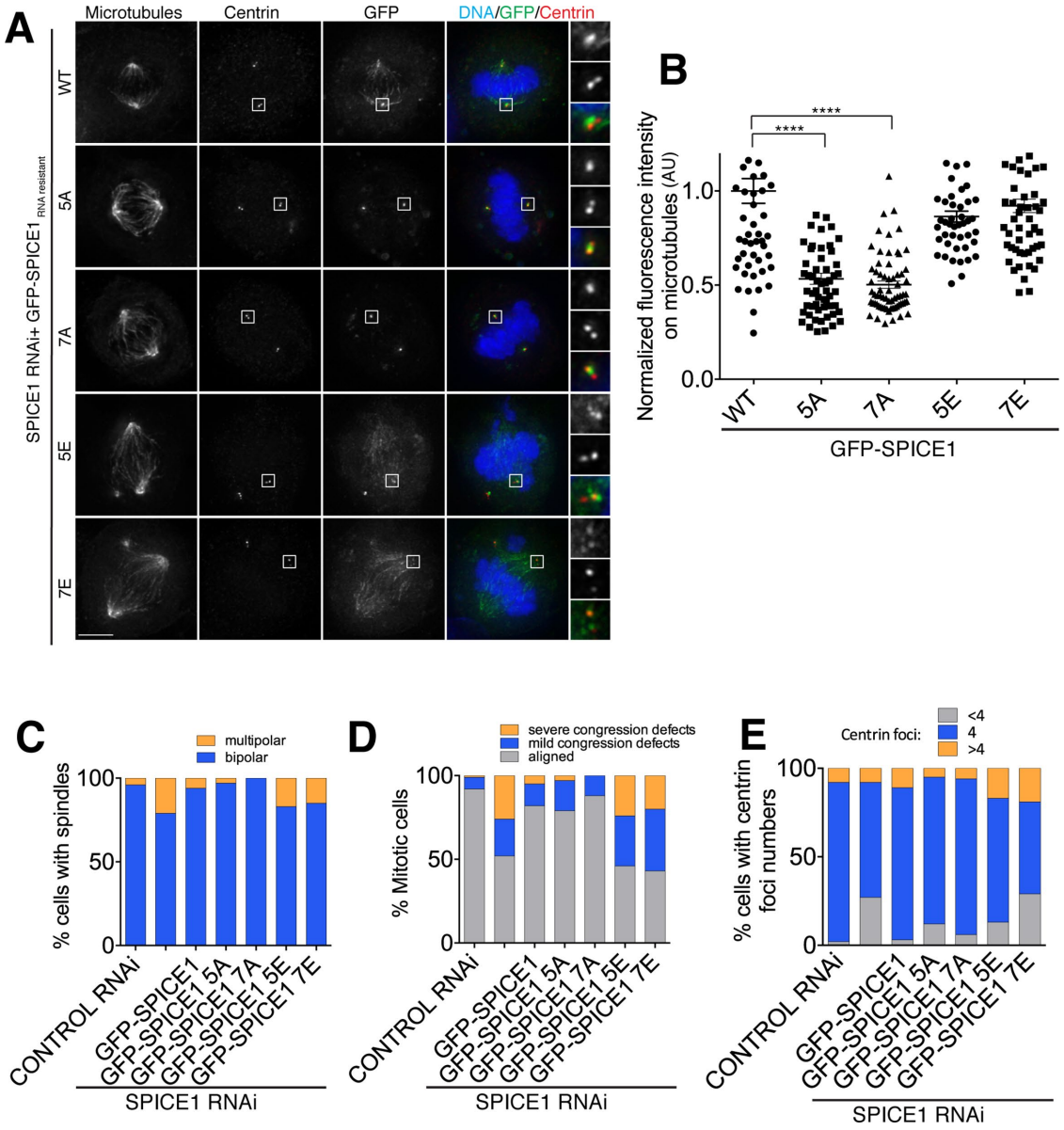

FIGURE 4: Constitutive phosphorylation of SPICE1 results in abnormal centriole number, chromosome alignment defects and spindle multipolarity. (A) Representative deconvolved immunofluorescent images showing the maximum projections of SPICE1-depleted HeLa cells transfected with GFP-SPICE1 mutants and costained with anti–β-tubulin and anti-centrin antibodies. (B) Scatter plot showing the average normalized GFP fluorescence intensity of SPICE1 mutants on microtubules relative to the fluorescence of GFP-SPICE1 on microtubules. The error bars represent the SEM. Experiment repeated twice (HeLa, WT $n = 55$; 5A $n = 57$; 7A $n = 66$; 5E $n = 46$; 7E $n = 58$). The p values for the one-way ANOVA test are reported: ****$p < 0.0001$. Scale bars, 5 μm. (C–E) Graphs showing quantifications of the percentage of cells with centriole defects, chromosome alignment defects, and spindle defects in HeLa cells depleted of endogenous SPICE1 while transiently expressing GFP-SPICE1 or GFP-tagged phosphorylation mutants. Measured in two experiments (control RNAi $n = 78$; SPICE RNAi $n = 77$; SPICE RNAi + SPICE1 WT $n = 63$; SPICE RNAi + $SPICE1_{5A}$ $n = 60$; SPICE RNAi + $SPICE1_{7A}$ $n = 66$; SPICE RNAi + $SPICE1_{5E}$ $n = 46$; SPICE RNAi + $SPICE1_{7E}$ $n = 59$).

Aurora A and Aurora B in vitro, showing that our computational approach to predict Aurora kinase phosphorylation sites is relevant and accurate. Very recently, Elys has been reported to have a protein phosphatase 1 (PP1)-binding motif (RV[S/Tp]F), phosphorylated by Aurora B, confirming our finding that Elys is an Aurora kinase substrate (Nasa *et al.*, 2018). Clasp2 is present at centrosomes, kinetochores, and microtubule plus ends, making it a prime candidate for Aurora kinase phosphorylation. Additionally, many of the predicted phosphorylation sites are localized in the glutamate-arginine–rich region phosphorylated by GSK3 (Kumar *et al.*, 2012). This region appears to regulate Clasp2 targeting to microtubules through disruption of two SXIP motifs and possibly through other mechanisms (Kumar *et al.*, 2012; Pemble *et al.*, 2017). Thus Aurora B phosphorylation of this region could provide a mitotic control of microtubule targeting. Many other Aurora substrates predicted in our database remain to be identified as such in vivo.

SPICE1 is implicated in centriole duplication and elongation, spindle integrity, and chromosome alignment (Archinti *et al.*, 2010;

Comartin *et al.*, 2013). While the SPICE1 N terminus contains the microtubule-binding region based on cellular localization (Archinti *et al.*, 2010) (Figure 2A), the C terminus appears as the regulatory region of the protein. Our results indicate that full-length SPICE1 overexpression results in abnormal centriole numbers with an increase in supernumerary centrioles (Figure 2, C and D). In the absence of the SPICE1 C terminus, cells overexpressing SPICE1 did not display any extra centrioles (Figure 2, C and D). Our analysis of SPICE1 regulation by Aurora kinases revealed that the C terminus of SPICE1 contains seven Aurora kinase phosphorylation sites. Mutants carrying the computationally predicted phosphorylation sites to alanines did not cause any cellular defects. Spindle architecture and centriole number was similar to that in control cells. SPICE1 nonphosphorylatable mutants did not localize to the spindle but remain present at centrioles, suggesting that SPICE1 centriole localization rather than spindle localization is important for maintaining centriole number. SPICE1 also promotes centriole elongation. However, it was not possible for us to measure centriole length in the presence of SPICE1 mutants, due to a lack of resolution of centrioles by conventional fluorescence microscopy.

The SPICE1 phosphomimetic mutant localized both to centrioles and spindles. Cells expressing a constitutive SPICE1 phosphomimetic mutant display spindle architecture defects, modest chromosome misalignment, and abnormal centriole number, reminiscent of SPICE1 depletion. Thus constitutive phosphorylation appears to interfere with SPICE1 function, possibly by allowing the N-terminal microtubule-binding region to associate with microtubules, in a noncontrolled manner. While the phosphorylation status of SPICE1 does not seem to regulate its centriole localization, centriole-localized SPICE1 may recruit proteins important to regulate centriole replication in an Aurora kinase-dependent manner. Consequently, the presence of phosphomimetic SPICE1 results in abnormal centriole regulation. Both an increase and a reduction in centriole number interfere with force balance in the spindle and can result in multipolarity (McKinley and Cheeseman, 2017). Multipolarity in turn can cause chromosome misalignment (Ganem *et al.*, 2009). Thus we believe that the SPICE1-induced centriole misregulation can cause the observed phenotype. Phosphorylation of SPICE1 promotes its association with the spindle (Figures 3 and 4). This could also interefere with microtubule dynamics, leading to spindle defects and chromosome misalignment. We conclude that dynamic phosphorylation of SPICE1 by Aurora kinases is necessary to maintain correct spindle architecture and centriole number. Aurora kinases are tethered to the centrosomes, chromosomes, and kinetochores. Cytoplasmic counteracting phosphatases are likely to dephosphorylate SPICE1 in a manner inversely proportional to its distance from the Aurora kinases to reduce the levels of SPICE1 on the spindle. We could not observe a localization gradient of SPICE1 after Aurora kinase inhibition. This could be due to the length of the inhibitor treatment, or the fixing conditions, which do not preserve the localization of weakly bound proteins to microtubules (Welburn and Cheeseman, 2012). Recently, in addition to its centrosome localization, Aurora A has been reported at kinetochores, which could explain the absence of SPICE1 localization gradient (DeLuca *et al.*, 2018; Eot-Houllier *et al.*, 2018). Further, molecular studies on SPICE1 are necessary to dissect the mechanism of SPICE1 in centriole and spindle function.

Overall, our computational approach reveals a rapid way to identify new Aurora kinase substrates and represents a user-friendly open-source tool for the community. Using this approach, we have identified multiple new Aurora kinase substrates in vitro and showed that SPICE1 is an Aurora kinase substrate both in vitro and in vivo, validating our approach.

MATERIALS AND METHODS

Cloning, protein expression, and purification

Genes of interest were PCR amplified from adult male testis or fetus brain cDNA library (Invitrogen) and inserted into pET3aTr and pBabe GFP blasticidin for bacterial expression and for transfections into human cells, respectively. Site-directed mutagenesis was performed using QuikChange (Agilent Technologies). Sequences were verified. A list of constructs and primers is provided in Table 1.

Recombinant proteins were expressed in BL21 (DE3) Codon plus cells with a His-tag preceded by 3C protease cleavage site. Protein expression and purification was performed as described (Talapatra *et al.*, 2015). To isolate the $KIAA1468_{1\text{-}292}$ fragment from the inclusion bodies and refold it, 100 ml of the cells expressing $KIAA1468_{1\text{-}292}$ was centrifuged, and cell pellets were resuspended in lysis buffer (50 mM Tris–HCl, pH 8.0, 100 mM NaCl, 1 mM EDTA, 0.5% Triton X-100, 10 mM dithiothreitol [DTT]). After repeated freeze–thaw cycles, the cell lysate was sonicated, and insoluble fraction was collected by centrifugation for 20 min at 15,000 rpm and 4°C. Inclusion bodies in pellet were washed three times with wash buffer (50 mM Tris–HCl, pH 8.0, 100 mM NaCl, 1 mM EDTA, 1% Triton X-100, 1 mM DTT), sonicated briefly, and pelleted at 15,000 rpm for 20 min at 4°C. Inclusion bodies were solubilized into 6 M Gdn–HCl, pH 4.5, and 5 mM β-mercaptoethanol (BME) stirring at room temperature. After solubilization, the buffer was exchanged with wash buffer (50 mM Tris–HCl, pH 8.0, 100 mM NaCl, 6 M urea, 10 mM imidazole, 5 mM BME) using desalting column (BioRad). The sample was then dialyzed against refolding buffer (50 mM Tris–HCl, pH 8.0, 100 mM NaCl, 4 M urea, 1 mM EDTA, 10% glycerol, 0.5 mM L-arginine) for 4 h at 4°C. The stepwise refolding continued with dialysis against the buffers with decreasing concentration of urea and finished with buffer without urea. The protein refolded properly without aggregation.

In vitro kinase assay and Western blotting

Purified recombinant protein fragments (2 µg) were incubated with 1.1 µg purified yeast recombinant glutathione-*S*-transferase–Ipl1, 0.2 µg human recombinant His-Aurora A (AMS Biotechnology Ltd.), or water in kinase buffer (150 mM NaCl, 40 mM HEPES, pH 7, 5 mM MgCl, 2 mM DTT, 20% glycerol) for 30 min at 37°C in the presence of 10 mM ATP and 5 µCi [γ-^{32}P] ATP. The kinase reaction mixtures were resuspended in SDS sample buffer and separated with 10% or 15% SDS–PAGE. To detect phosphorylation, dried gels were exposed to an x-ray film (Fuji-Film). Simultaneously, same samples were prepared without [γ-^{32}P] ATP and run out with SDS–PAGE, and gels were stained with Coomassie Brilliant Blue. For Western blotting, HeLa cells were lysed in SDS sample buffer and equal amount of cell extract per lane were loaded into a SDS–PAGE gel, run out, transferred to a nitrocellulose membrane, and blotted with rabbit anti-SPICE1 (HPA064843; Atlas Antibodies) and mouse anti–β-tubulin (Sigma) as loading control.

Cell culture and microscopy

Cells were maintained in DMEM (Lonza) supplemented with 10% fetal bovine serum penicillin/streptomycin (Life Technologies) at 37°C in a humidified atmosphere with 5% CO_2. Cells were checked monthly for mycoplasma contamination (Mycoalert kit; Lonza). Cells were plated on 18-mm glass coverslips coated with poly-L-lysine (Sigma-Aldrich) for immunostaining. Transient transfections of DNA were conducted using Effectene reagent (Qiagen) according to the manufacturer's guidelines. RNAi experiments were conducted using jetPRIME transfection reagent (Polyplus) according to the manufacturer's protocol. Previously published siRNA oligo was used to

Amplification from cDNA library	Primer sequence			
Full-length ELYS	GTGGAACTCGGTTTTGTCGG			
	CCTGGACTGAAACAATCACTCC			
Full-length TTLL4	CAGACTGACAGACTTCAAGGATGC			
	AGGCTTTTGGAGAGAGGCCAG			
Full-length SPICE1	CTGTGTTTTGAGAGTGCAAGTACG			
	GAACAAACTCAGTGAGACTTGACTTC			
Bacterial expression	**Primer sequence**	**Vector**	**Enzymes/method**	**Template**
ELYS$_{1858-2014}$-3C protease cleavage site-6xHis	gaaggagatatacatatgACTAAAAAAGAAGTTAAGGTTTCATC	pET3aTr	*Nde*I/Gibson assembly	ELYS isoform 2 NP_001310271.1
	ccaagcttagatctggatccTCAGTGGTGATGATGATGATGGCTGCTGCCGGGCCCCTGGAACAGAACTTCCAGTGGGGTATTTCTTGTAGATCTCC	pET3aTr	*Bam*HI/Gibson assembly	ELYS isoform 2 NP_001310271.1
CLASP2$_{741-818}$-3C protease cleavage site-6xHis	gaaggagatatacatatgCCATCTAGGCTTTCAGTGGC	pET3aTr	*Nde*I/Gibson assembly	CLASP2 isoform X15 XP_006713112.1
	ccaagcttagatctggatccTCAGTGGTGATGATGATGATGGCTGCTGCCGGGCCCCTGGAACAGAACTTCCAGAGAAGACGACAGTCGACTTGATTG	pET3aTr	*Bam*HI/Gibson assembly	CLASP2 isoform X15 XP_006713112.1
SPICE1$_{549-855}$-3C protease cleavage site-6xHis	tttaagaaggagatatacatatgCCTCTTCAGGACGTATTGAG	pET3aTr	*Nde*I/Gibson assembly	SPICE1 isoform a NP_001318007.1
	ccaagcttagatctggatccTCAGTGGTGATGATGATGATGGCTGCTGCCGGGCCCCTGGAACAGAACTTCCAGTGATACATGGGTAGAAAGAGCA	pET3aTr	*Bam*HI/Gibson assembly	SPICE1 isoform a NP_001318007.1
TTLL4$_{330-624}$-3C protease cleavage site-6xHis	tttaagaaggagatatacatatgCCAACTAAGGAGATTCGGTTC	pET3aTr	*Nde*I/Gibson assembly	TTLL4 NP_055455.3
	ccaagcttagatctggatccTCAGTGGTGATGATGATGATGGCTGCTGCCGGGCCCCTGGAACAGAACTTCCAGTCCAATGGTCTGCTTGACAATG	pET3aTr	*Bam*HI/Gibson assembly	TTLL4 NP_055455.3
KIAA1468$_{1-292}$-3C protease cleavage site-6xHis	tttaagaaggagatatacatatgTTAGTACAGAAATTAGAAGATAAAATTAGTTTG	pET3aTr	*Nde*I/Gibson assembly	KIAA1468 isoform CRA_a EAW63120.1
	ccaagcttagatctggatccTCAGTGGTGATGATGATGATGGCTGCTGCCGGGCCCCTGGAACAGAACTTCCAGTAACATTTGTTGCAACATTGAAAG	pET3aTr	*Bam*HI/Gibson assembly	KIAA1468 isoform CRA_a EAW63120.1
Mammalian expression	**Primer sequence**	**Vector**	**Enzymes/method**	**Template**
Full-length GFP-SPICE1	cccgCTCGAGATGTCATTTGTCAGAGTGAACCGCT	pBabe blast	*Xho*I	Isoform a NP_001318007.1
	tcccCCGCGGTTATGATACATGGGTAGAAAGAGCAAAC	pBabe blast	*Sac*II	Isoform a NP_001318007.1
GFP-SPICE1$_{444-855}$	cccCTCGAGATATCACTCACACATGCTATTAAGAACT	pBabe blast	*Xho*I	Isoform a NP_001318007.1
GFP-SPICE1$_{1-550}$	tcccCCGCGGTTAAAGAGGAGAGAATTTTAAGT	pBabe blast	*Sac*II	Isoform a NP_001318007.1
Mutagenesis	**Primer sequence**			
GFP-SPICE1 hd 1st 5 bases	CTCCCAGTACTGGGAGATGGGCAGCAATTAAGGACTAATGAGTCATTAATACAAAGAAAGGAC			

TABLE 1: Details of constructs generated and primer sequences.

Continues

	GTCCTTTCTTTGTATTAATGACTCATTAGTCCT-TAATTGCTGCCCATCTCCCAGTACTGGGAG
GFP-SPICE1 hd 2nd 5 bases	CTGGGAGATGGGCAGCAATTAAGGACTA-ACGAAAGTTTAATACAAAGAAAGGACATAAT-GACACG
	CGTGTCATTATGTCCTTTCTTTGTAT-TAAACTTTCGTTAGTCCTTAATTGCT-GCCCATCTCCCAG
GFP-SPICE1 T557A	AGGACGTATTGAGAAGGGCTGTTCAAACTC-GTCCT
	AGGACGAGTTTGAACAGCCCTTCTCAATAC-GTCCT
GFP-SPICE1 S738A	TTGCAGAATTGAATCGACAAGCTATGGAG-GCTCGTGGAAAAC
	GTTTTCCACGAGCCTCCATAGCTTGTC-GATTCAATTCTGCAA
GFP-SPICE1 T780A	GACTGAAGGAGCAAAGAGGGCAATTGAGG-TATCTATTCC
	GGAATAGATACCTCAATTGCCCTCTTT-GCTCCTTCAGTC
GFP-SPICE1 S797A	CCCAGAAAGCTCAAAATGTGCTACT-GTCTCTCCCGTCAGC
	GCTGACGGGAGAGACAGTAGCACATTTT-GAGCTTTCTGGG
GFP-SPICE1 S810A Forward	GCGGGATAAATACAAGAAGAGCTTCCG GGGCTACT
	AGTAGCCCCGGAAGCTCTTCTTGTATTTATCCC-GC
GFP-SPICE1 S797A/ T798A	GCCCCAGAAAGCTCAAAATGTGCTGCT-GTCTCTCCCGTCAG
	CTGACGGGAGAGACAGCAGCACATTTT-GAGCTTTCTGGGGC
GFP-SPICE1 S810A/ S811A	TCAGCGGGATAAATACAAGAAGAGCTGCC-GGGGCTACTG
	CAGTAGCCCCGGCAGCTCTTCTTGTATT-TATCCCGCTGA
GFP-SPICE1 T557E	CTTCAGGACGTATTGAGA-AGGGAAGTTCAAACTCGTCCTGCTCCA
	TGGAGCAGGACGAGTTTGAACTTCCCTTCT-CAATACGTCCTGAAG
GFP-SPICE1 S738E	GGAACGGATTGCAGAATTGAATCGA-CAAGAAATGGAGGCTCGTGGA
	TCCACGAGCCTCCATTTCTTGTC-GATTCAATTCTGCAATCCGTTCC
GFP-SPICE1 T780E	GGACTGAAGGAGCAAAGAGGGAAATTGAG-GTATCTATTCCAG
	CTGGAATAGATACCTCAATTTCCCTCTTT-GCTCCTTCAGTCC
GFP-SPICE1 S797E	GCAGAAGCCCCAGAAAGCTCAAAATGT-GAAACTGTCTCTCCCGT
	ACGGGAGAGACAGTTTCACATTTT-GAGCTTTCTGGGGCTTCTGC

TABLE 1: Details of constructs generated and primer sequences.

Continues

GFP-SPICE1 S810E	CCCGTCAGCGGGATAAATACAAGAAGAGA-ATCCGGGGCTACTGG		
	CCAGTAGCCCCGGATTCTCTTCTTGTATT-TATCCCGCTGACGGG		
GFP-SPICE1 S797E/ T798E	GGAGCAGAAGCCCCAGAAAGCTCAAAATGT-GAAGAAGTCTCTCCCGTCAGCGGGA		
	TCCCGCTGACGGGAGAGACTTCTTCACATTTT-GAGCTTTCTGGGGCTTCTGCTCC		
GFP-SPICE1 S810E/ S811E	AGAAGTCTCTCCCGTCAGCGGGATAAATACAA GAAGAGAAGAGGGGGCTACTGGTAATTCTT		
	AAGAATTACCAGTAGCCCCCTCTTCTCTTCTTG-TATTTATCCCGCTGACGGGAGAGACTTCT		
CRISPR Cas9	**Oligo sequence**	**Vector**	**Enzymes/method**
guide RNA targeting exon3 in *SPICE1* gene	[phospho]caccgTTCGGGAGTTGCCCGATGAA	pLentisgRNA	*Bbs*I
	[phospho]aaacTTCATCGGGCAACTCCCGAAc	pLentisgRNA	*Bbs*I

TABLE 1: Details of constructs generated and primer sequences. Continued

deplete SPICE1 (Archinti *et al.*, 2010). The cells were visualized 48 h after transfection or cotransfection.

The inducible SPICE1 knockout (KO) cell line was generated as previously described (McKinley *et al.*, 2015; Wang *et al.*, 2016) using guide RNA (gRNA) 5′-TTCGGGAGTTGCCCGATGAA-3′, targeting exon 3 of *SPICE1*. KO was introduced with 1 μg/ml doxycycline (Sigma) treatment of stable HeLa $Cas9_{SPICE1\ gRNA}$ cells for 96 h. For Aurora kinase inhibition experiments, HeLa cells were incubated for 1.5 h with small molecule inhibitors at the following concentrations: ZM447439, 2 μM; MLN8237, 150 nM (Selleckchem).

Immunofluorescence in human cells was conducted as previously described (Welburn *et al.*, 2010) using antibodies against mouse anti-tubulin (Sigma), rabbit anti-Centrin (Covance; custom-made), and rabbit α-SPICE1 (HPA064843; Atlas Antibodies). Images were acquired on a DeltaVision Core deconvolution microscope (Applied Precision) equipped with a CoolSnap HQ2 CCD camera. Thirty Z-sections were acquired at 0.2-nm steps using a 100×/1.3 NA Olympus U-PlanApo objective without binning. Equivalent exposure conditions were used between controls and drug-treated cells in a single experiment, as well as in case of nontransfected cells and cells transfected with different constructs. On average, experiments were repeated three times. To quantitate GFP fluorescence intensity, at least 10 individual MT as polylines of 35–37 pixels in size were selected from projections (selected based on colocalization with β-tubulin) and the integrated intensity was determined after subtracting the average background fluorescence measured from adjacent regions of the cell (two polylines form inside and two from outside the spindle) using Metamorph. To quantify chromosome congression defects in SPICE1 knockdown and KO, the cells were scored as having congressed chromosome, mild congression defects, and severe congression defects based on Hoechst staining. The cells with at least five misaligned chromosomes were scored as mild congression defects; the cells with more than five misaligned chromosomes as cells with severe defects. To quantify spindle morphology defects, the cells were scored as having bipolar or multipolar spindle based on β-tubulin staining and spindle morphology. To quantify defects in centriole numbers, the cells were scored as having <4, 4, and >4 centrioles based on centrin staining. Integrated intensities of pS10-H3 signals were measured from chromatin surface (based on Hoechst staining) using Image-Pro-Premier software (Media Cybernetics).

Images were stored and vizualised using an OMERO.insight client (Linkert *et al.*, 2010).

Statistics and reproducibility

Statistical analyses were performed using GraphPad Prism 6.0 or R software. No statistical method was used to predetermine sample size. No samples were excluded from the analyses. All experiments were performed and quantified from at least three independent experiments, unless specified, and the representative data are shown.

Statistical analysis of data was performed with GraphPad Prims using Student's *t* test, one-way analysis of variance (ANOVA) tests, and nonparametric tests. A Kolmogorov–Smirnov test was used to test variation in centriole number (Figure 2D), which had a non-Gaussian distribution.

Data availability

All data supporting the findings of this study are available from the corresponding author on request.

Software

fuzzpro from the EMBOSS suite (version 6.6.0.0) was used to find matches to patterns in each of the three peptide data sets (Rice *et al.*, 2000). Needle from the same suite was used to calculate the percentage identity between all possible pairwise regions that contained pattern matches in orthologous proteins, and the highest identity per pair was recorded. *iupred* (Dosztanyi *et al.*, 2005) was used to calculate the likelihood for an amino acid regions present in a disordered region. Amino acids that have values larger than 0.5 were counted within regions containing a pattern match. *samtools* (version 0.1.19) was used to both index and retrieve sequences from the fasta files (Li *et al.*, 2009).

Shiny application

The R-Shiny application can be launched in any R session with an installed shiny package using the commands

library (shiny)
runGitHub ("DereticWelburnApp," "AlastairKerr")

The interface produces a table for proteins that match at least one of the prosite patterns in each of the three orthologues.

Prosite patterns used are

pattern 1 "[RK][RK]x[TS][FAST]"

pattern 2 "[RK][RK]x[TS][ILVM]"

pattern 3 "x[RK][RK][TS][FAST]"

pattern 4 "x[RK][RK][TS][ILVM]"

pattern 5 "[RK][RK][RK][TS][ILVM]"

pattern 6 "[RK][RK][RK][TS][FAST]"

Additional filters can be applied to the number of pattern matches in a set protein region, data based on the percentage of amino acids predicted to be in disorder in the region, the maximum identity between two pattern containing regions in orthologous proteins, and annotations to select Gene Ontology terms or mitosis pathways.

The code is available at the links below:

https://github.com/AlastairKerr/DereticWelburnPreprocessingScripts

All code that was used for preprocessing the data as well as the r-shiny application is available on github.

Preprocessing: https://github.com/AlastairKerr/DereticWelburnPreprocessingScripts

R-Shiny application: https://github.com/AlastairKerr/DereticWelburnApp

The phosphorylation search database is also found at http://bifx-rta.bio.ed.ac.uk:3838/Welburn/Patterns_Regions/

ACKNOWLEDGMENTS

We thank members of the Welburn lab for critical reading of the manuscript. J.W. is supported by a Wellcome Trust Senior Research Fellowship (Grant No. 207430). The Wellcome Trust Centre for Cell Biology and A. Kerr are supported by core funding from the Wellcome Trust (203149).

REFERENCES

Andrews PD, Ovechkina Y, Morrice N, Wagenbach M, Duncan K, Wordeman L, Swedlow JR (2004). Aurora B regulates MCAK at the mitotic centromere. Dev Cell 6, 253–268.

Archinti M, Lacasa C, Teixido-Travesa N, Luders J (2010). SPICE–a previously uncharacterized protein required for centriole duplication and mitotic chromosome congression. J Cell Sci 123, 3039–3046.

Bailey TL, Boden M, Buske FA, Frith M, Grant CE, Clementi L, Ren J, Li WW, Noble WS (2009). MEME suite: tools for motif discovery and searching. Nucleic Acids Res 37, W202–W208.

Bishop JD, Schumacher JM (2002). Phosphorylation of the carboxyl terminus of inner centromere protein (INCENP) by the Aurora B kinase stimulates Aurora B kinase activity. J Biol Chem 277, 27577–27580.

Cheeseman IM, Anderson S, Jwa M, Green EM, Kang J, Yates JR 3rd, Chan CS, Drubin DG, Barnes G (2002). Phospho-regulation of kinetochore-microtubule attachments by the Aurora kinase Ipl1p. Cell 111, 163–172.

Cheeseman IM, Chappie JS, Wilson-Kubalek EM, Desai A (2006). The conserved KMN network constitutes the core microtubule-binding site of the kinetochore. Cell 127, 983–997.

Ciferri C, Pasqualato S, Screpanti E, Varetti G, Santaguida S, Dos Reis G, Maiolica A, Polka J, De Luca JG, De Wulf P, *et al.* (2008). Implications for kinetochore-microtubule attachment from the structure of an engineered Ndc80 complex. Cell 133, 427–439.

Comartin D, Gupta GD, Fussner E, Coyaud E, Hasegan M, Archinti M, Cheung SW, Pinchev D, Lawo S, Raught B, *et al.* (2013). CEP120 and SPICE1 cooperate with CPAP in centriole elongation. Curr Biol 23, 1360–1366.

de Groot CO, Hsia JE, Anzola JV, Motamedi A, Yoon M, Wong YL, Jenkins D, Lee HJ, Martinez MB, Davis RL, *et al.* (2015). A cell biologist's field guide to aurora kinase inhibitors. Front Oncol 5, 285.

DeLuca JG, Gall WE, Ciferri C, Cimini D, Musacchio A, Salmon ED (2006). Kinetochore microtubule dynamics and attachment stability are regulated by Hec1. Cell 127, 969–982.

DeLuca KF, Meppelink A, Broad AJ, Mick JE, Peersen OB, Pektas S, Lens SMA, DeLuca JG (2018). Aurora A kinase phosphorylates Hec1 to regulate metaphase kinetochore-microtubule dynamics. J Cell Biol 217, 163–177.

Dephoure N, Zhou C, Villen J, Beausoleil SA, Bakalarski CE, Elledge SJ, Gygi SP (2008). A quantitative atlas of mitotic phosphorylation. Proc Natl Acad Sci USA 105, 10762–10767.

Dosztanyi Z, Csizmok V, Tompa P, Simon I (2005). The pairwise energy content estimated from amino acid composition discriminates between folded and intrinsically unstructured proteins. J Mol Biol 347, 827–839.

Dulla K, Daub H, Hornberger R, Nigg EA, Korner R (2010). Quantitative site-specific phosphorylation dynamics of human protein kinases during mitotic progression. Mol Cell Proteomics 9, 1167–1181.

Eot-Houllier G, Magnaghi-Jaulin L, Fulcrand G, Moyroud F-X, Monier S, Jaulin C (2018). Aurora A-dependent CENP-A phosphorylation at inner centromeres protects bioriented chromosomes against cohesion fatigue. Nat Commun 9, 1888.

Fu J, Bian M, Liu J, Jiang Q, Zhang C (2009). A single amino acid change converts Aurora-A into Aurora-B-like kinase in terms of partner specificity and cellular function. Proc Natl Acad Sci USA 106, 6939–6944.

Fu J, Bian M, Xin G, Deng Z, Luo J, Guo X, Chen H, Wang Y, Jiang Q, Zhang C (2015). TPX2 phosphorylation maintains metaphase spindle length by regulating microtubule flux. J Cell Biol 210, 373–383.

Gallini S, Carminati M, De Mattia F, Pirovano L, Martini E, Oldani A, Asteriti IA, Guarguaglini G, Mapelli M (2016). NuMA phosphorylation by aurora-A orchestrates spindle orientation. Curr Biol 26, 458–469.

Ganem NJ, Godinho SA, Pellman D (2009). A mechanism linking extra centrosomes to chromosomal instability. Nature 460, 278–282.

Hans F, Skoufias DA, Dimitrov S, Margolis RL (2009). Molecular distinctions between Aurora A and B: a single residue change transforms Aurora A into correctly localized and functional Aurora B. Mol Biol Cell 20, 3491–3502.

Honda R, Korner R, Nigg EA (2003). Exploring the functional interactions between Aurora B, INCENP, and survivin in mitosis. Mol Biol Cell 14, 3325–3341.

Hornbeck PV, Zhang B, Murray B, Kornhauser JM, Latham V, Skrzypek E (2015). PhosphoSitePlus, 2014: mutations, PTMs and recalibrations. Nucleic Acids Res 43, D512–D520.

Kettenbach AN, Schweppe DK, Faherty BK, Pechenick D, Pletnev AA, Gerber SA (2011). Quantitative phosphoproteomics identifies substrates and functional modules of Aurora and Polo-like kinase activities in mitotic cells. Sci Signal 4, rs5.

Kim Y, Holland AJ, Lan W, Cleveland DW (2010). Aurora kinases and protein phosphatase 1 mediate chromosome congression through regulation of CENP-E. Cell 142, 444–455.

Kumar P, Chimenti MS, Pemble H, Schonichen A, Thompson O, Jacobson MP, Wittmann T (2012). Multisite phosphorylation disrupts arginine-glutamate salt bridge networks required for binding of cytoplasmic linker-associated protein 2 (CLASP2) to end-binding protein 1 (EB1). J Biol Chem 287, 17050–17064.

Kumar P, Wittmann T (2012). +TIPs: SxIPping along microtubule ends. Trends Cell Biol 22, 418–428.

Li H, Handsaker B, Wysoker A, Fennell T, Ruan J, Homer N, Marth G, Abecasis G, Durbin R, S. Genome Project Data Processing (2009). The sequence alignment/map format and SAMtools. Bioinformatics 25, 2078–2079.

Linkert M, Rueden CT, Allan C, Burel JM, Moore W, Patterson A, Loranger B, Moore J, Neves C, Macdonald D, *et al.* (2010). Metadata matters: access to image data in the real world. J Cell Biol 189, 777–782.

McKinley KL, Cheeseman IM (2014). Polo-like kinase 1 licenses CENP-A deposition at centromeres. Cell 158, 397–411.

McKinley KL, Cheeseman IM (2017). Large-scale analysis of CRISPR/Cas9 cell-cycle knockouts reveals the diversity of p53-dependent responses to cell-cycle defects. Dev Cell 40, 405–420 e402.

McKinley KL, Sekulic N, Guo LY, Tsinman T, Black BE, Cheeseman IM (2015). The CENP-L-N complex forms a critical node in an integrated meshwork of interactions at the centromere-kinetochore interface. Mol Cell 60, 886–898.

Mok J, Kim PM, Lam HY, Piccirillo S, Zhou X, Jeschke GR, Sheridan DL, Parker SA, Desai V, Jwa M, *et al.* (2010). Deciphering protein kinase specificity through large-scale analysis of yeast phosphorylation site motifs. Sci Signal 3, ra12.

Moritz A, Li Y, Guo A, Villen J, Wang Y, MacNeill J, Kornhauser J, Sprott K, Zhou J, Possemato A, *et al*. (2010). Akt-RSK-S6 kinase signaling networks activated by oncogenic receptor tyrosine kinases. Sci Signal 3, ra64.

Nasa I, Rusin SF, Kettenbach AN, Moorhead GB (2018). Aurora B opposes PP1 function in mitosis by phosphorylating the conserved PP1-binding RVxF motif in PP1 regulatory proteins. Sci Signal 11, eaai8669.

Okada M, Cheeseman IM, Hori T, Okawa K, McLeod IX, Yates JR 3rd, Desai A, Fukagawa T (2006). The CENP-H-I complex is required for the efficient incorporation of newly synthesized CENP-A into centromeres. Nat Cell Biol 8, 446–457.

Olsen JV, Vermeulen M, Santamaria A, Kumar C, Miller ML, Jensen LJ, Gnad F, Cox J, Jensen TS, Nigg EA, *et al*. (2010). Quantitative phosphoproteomics reveals widespread full phosphorylation site occupancy during mitosis. Sci Signal 3, ra3.

Pemble H, Kumar P, van Haren J, Wittmann T (2017). GSK3-mediated CLASP2 phosphorylation modulates kinetochore dynamics. J Cell Sci 130, 1404–1412.

Rice P, Longden I, Bleasby A (2000). EMBOSS: the European Molecular Biology Open Software Suite. Trends Genet 16, 276–277.

Santamaria A, Wang B, Elowe S, Malik R, Zhang F, Bauer M, Schmidt A, Sillje HH, Korner R, Nigg EA (2011). The Plk1-dependent phosphoproteome of the early mitotic spindle. Mol Cell Proteomics 10, M110 004457.

Talapatra SK, Harker B, Welburn JP (2015). The C-terminal region of the motor protein MCAK controls its structure and activity through a conformational switch. Elife 4, e06421.

Wang T, Lander ES, Sabatini DM (2016). Single guide RNA library design and construction. Cold Spring Harb Protoc 2016, prot090803.

Welburn JP, Cheeseman IM (2012). The microtubule-binding protein Cep170 promotes the targeting of the kinesin-13 depolymerase Kif2b to the mitotic spindle. Mol Biol Cell 23, 4786–4795.

Welburn JP, Vleugel M, Liu D, Yates JR 3rd, Lampson MA, Fukagawa T, Cheeseman IM (2010). Aurora B phosphorylates spatially distinct targets to differentially regulate the kinetochore-microtubule interface. Mol Cell 38, 383–392.

Welburn JPI, Jeyaprakash AA (2018). Mechanisms of mitotic kinase regulation: a structural perspective. Front Cell Dev Biol 6, 6.

Ye AA, Deretic J, Hoel CM, Hinman AW, Cimini D, Welburn JP, Maresca TJ (2015). Aurora a kinase contributes to a pole-based error correction pathway. Curr Biol 25, 1842–1851.

Zaytsev AV, Mick JE, Maslennikov E, Nikashin B, DeLuca JG, Grishchuk EL (2015). Multisite phosphorylation of the NDC80 complex gradually tunes its microtubule-binding affinity. Mol Biol Cell 26, 1829–1844.

Zhang X, Ems-McClung SC, Walczak CE (2008). Aurora A phosphorylates MCAK to control ran-dependent spindle bipolarity. Mol Biol Cell 19, 2752–2765.